

Proposed X-ray scattering beamlines at NSLS-II for life sciences research

The life science research community at NSLS has been discussing the transition to NSLS-II for some time. In 2008, a NSLS strategic planning workshop was held at BNL and a white paper was generated (see <http://www.bnl.gov/lis/workshops.asp>). This white paper expressed the community's desire to fully take advantage of the NSLS-II source brightness to perform cutting edge X-ray scattering experiments, at the same time to be able to continue to perform routine X-ray solution measurements, which have been increasingly more frequently used in structural biology research in recent years.

NSLS-II recently announced the call for beamline development proposals (<http://www.bnl.gov/nsls2/2010BeamlineProposals.asp>). In response, we have submitted two Letters of Intent (LOIs, see Appendix I) to NSLS-II for proposals for two instruments: a high brightness X-ray scattering instrument and a high throughput one dedicated to solution scattering. This document, as a follow-up to the whitepaper, describes the baseline specifications of the instruments and the expected performances.

1. High brightness X-ray scattering instrument

As described in the white paper, the scientific programs enabled by the source brightness at NSLS-II include (1) following the structural evolution (e.g. folding, ligand-induced structural change) of biomolecules in solution using microfluidic flow cells; (2) probing the structure of membrane proteins and the membrane itself in single-layered, planar lipid membranes; (3) monitoring the hierarchical structures in biological tissues, such as the organic-inorganic composite bone structure and the organization of collagen in tissues, in a spatially resolved and/or time-resolved fashion.

All of these three scientific areas will require high source brightness. The instrument therefore will be based on an undulator source and utilize photon-counting pixel array detectors that are free of electronic noise and can handle high per-pixel count rate (>10k counts/sec) and high frame rate (>30 frames/sec). Yet each one will require the instrument to operate in a specialized configuration. It is therefore necessary to switch quickly from one configuration to another. The X9 beamline at NSLS provides a good example of the capability to accommodate multiple configurations (see Appendix II) and will serve as a prototype for the new instrument. The baseline specification and the estimated performance for each configuration, based on a beamline layout similar to X9 (see discussion in Appendices III-V), are summarized below.

A. Time-resolved X-ray scattering using microfluidic flow cells

- Transmission SAXS/WAXS
- X-ray energy: 12keV
- Spot size: 25 micron (H, FWHM) x 5 micron (V, full size)
- Combined q -range: 0.005-2.5 Å⁻¹ (4mm diameter beamstop at 2.5m)
- Flux at the sample: $\sim 2.4 \times 10^{13}$ photons/sec/0.01%bw

The aim of this configuration is to perform X-ray scattering measurement on flow cells similar to those used in fluorescence measurements, with time resolution approaching 10 microsecond. For instance, the flow cell described by Bilsel *et.al.*¹ can achieve time resolution of $\sim 50\mu\text{s}/\text{mm}$ (at 10ml/min flow rate, 75 μm channel width). To do so, a small beam spot with near-rectangular profile is required at the sample. At the same time the divergence of the beam will be kept low to allow access to small scattering angles. This will be accomplished using a secondary source, whose size and shape is defined by slits (see Appendix III).

B. Membrane structures

- Grazing incident SAXS/WAXS
- X-ray energy: 2.1keV - 20keV
 - Up to 20keV to provide X-ray penetration though bulk water under which the membrane structure is maintained.
 - 2.1keV to provide access to absorption edge of phosphorous (for structures that are not buried under water).
- Spot size: 0.2mm (H) x 1 micron (V) (FWHM); depth of focus $\sim 1\text{cm}$
- Combined q -range (in-plane): $0.005\text{-}2.5\text{\AA}^{-1}$ (4mm wide beamstop at 2.5m)
- Capability to measure X-ray reflectivity
- Flux at the sample @12keV: 4.1×10^{12} photons/sec/0.01%bw

The possibility of using X-ray scattering to study substrate-supported single bilayer has just emerged in recent years (see e.g. Yang *et.al.*² for an example). This methods can potentially be adapted to become the membrane protein equivalent of solution scattering, by reconstituting membrane proteins into the supported lipid bilayer. In such structures, the membrane proteins exist in the bilayer in a 2D solution-like state and the electron density contrast of membrane protein against the lipid bilayer produces X-ray scattering signal. The scattering data can be compared to calculated scattering intensity, for instance by using the few but growing number of existing membrane protein crystal structures, to validate the crystal structure and to determine the location and orientation of the membrane protein inside the bilayer. The crystal structure can also be used to elucidate conformation change in the membrane protein, such as when a ligand is bound or freed, based on rigid body modeling of the scattering data.

For these measurements to become practical, the background scattering from the bulk water, under which the membrane structure is maintained, must be minimized. The small vertical beam size in this configuration will help to reduce the volume of bulk water that contributes to the scattering signal, therefore minimize the background scattering.

C. Biological hierarchical structures

¹ O. Bilsel *et.al.*, "A microchannel solution mixer for studying microsecond protein folding reactions", *Rev. Sci. Instr.*, 76:014302, 2005

² L. Yang *et.al.* "Structure and interaction in 2D assemblies of tobacco mosaic viruses", *Soft Matter*, 5:4951, 2009

- Transmission SAXS/WAXS
- X-ray energy: up to 20keV to provide X-ray penetration through the sample
- Spot size: as small as 1 micron x 1 micron (FWHM)
- Combined q -range: 0.0005 - 2.5 \AA^{-1} (depending on the focus size)
- The WAXS detector should cover all azimuthal angles in reciprocal space, with variable sample-to-detector distance.
- High resolution in-line optical microscope to help visualize the sample.
- Flux at the sample @ 12keV: 1.2×10^{12} photons/sec/0.01%bw

This new instrument will have the capability of scanning probe imaging based on X-ray scattering data (see e.g. review by Paris³ for a description of this method), for visualizing the structural textures within biological tissues such as bones. The beam size in this imaging mode will be adjustable based on user requirement and as small as 1 micron x 1 micron, again by utilizing a slits-defined secondary source and a variety of secondary focusing optics. For measurements that require access to very low q , the beam size will be relaxed, or the divergence of the X-ray beam will be reduced at the expense of the X-ray flux.

2. High throughput X-ray scattering instrument

This instrument will be dedicated to static, simultaneous SAXS/WAXS measurements of biomolecules in solution (see Appendix II for an example of SAXS/WAXS data collected at X9). Sample handling, data collection and data processing on this instrument will be highly automated. In addition, optical spectroscopy characterization, including light scattering, UV-Vis and CD can be performed, using commercial HPLC detectors, in series with X-ray scattering measurement for each sample. In-line sample purification will also be available.

These source-independent capabilities are currently being developed at beamline X9 at NSLS. For samples that require optical spectroscopy measurements, a liquid handling device will be used to flow sample through multiple devices, including the cell for X-ray measurement, at an estimated rate of ~ 10 samples per hour (need to check) without interruption, as limited by the time needed to flow the sample through all devices and cleaning. For samples that require X-ray scattering measurements only, a multiple-cell sample changer will be used to accomplish ~ 60 samples per hour. The instrumentation developed at X9 can be transferred to NSLS-II when the new instrument is built.

This high throughput instrument will utilize either a three-pole wiggler or a short undulator source, operating at a fixed X-ray energy. A multilayer monochromator with wide energy band pass ($\sim 1\%$) will be used to improve the flux performance of the instrument. The baseline specifications of this instrument and the estimated performance are listed below:

- Transmission SAXS/WAXS
- X-ray energy: 12keV (fixed)

³ O. Paris, "From diffraction to imaging", *Biointerphases*, 3(2):FB16, 2008

- Spot size: 0.5mm x 0.2mm
- Camera length: 2.5m (SAXS) and 0.4m (WAXS)
- Combined q-range: 0.004-2.5 Å⁻¹
- Flux at the sample (TPW): 1.8 x 10¹² photon/sec/1%bw
- Flux at the sample (short ID): 1.6 x 10¹² photon/sec/0.01%bw

The ability to quickly and automatically measure a large number of samples will allow users to easily perform titration series and library-based screening. From the point of view of beamline operations, access to the instrument will be very flexible. For instance, multiple user groups can share access of the instrument, with one group measuring the samples while the others preparing the samples. Access via a mail-in service will also be offered to users that require frequent access to X-ray scattering measurements or cannot travel to the beamline for the experiments.

Appendix I. LOIs submitted to NSLS-II

NSLS-II Beamline Letter of Intent

Title	A high brightness X-ray scattering instrument for biological applications
Science Program	The scientific program at this beamline will have three major themes: (1) Structural dynamics of biological molecules in solution on microsecond to sub-second time scale (2) Structure characterization of membrane proteins in planar lipid membrane (3) Scanning probe mapping of organic matrices in biological tissues.
Beamline Description	Transmission and grazing incidence X-ray scattering with tunable beam size and divergence using an undulator source (high beta).
Proposal Type	Type 1

Proposal Team (the membership is expected to evolve as the proposal is being developed)

Lin Yang (Spokesperson)
Scientist
National Synchrotron Light Source
Brookhaven National Laboratory
Upton, NY 11973
Phone: (631) 344-5833
E-mail: lyang@bnl.gov

Marc Allaire
Biophysicist
National Synchrotron Light Source
Brookhaven National Laboratory
Upton, NY 11973
Phone: (631) 344-4795
E-mail: allaire@bnl.gov

Zimei Bu
Associate Member
Fox Chase Cancer Center
Reimann 414, 333 Cottman Ave
Philadelphia, PA 19111-2434
Phone: (215) 728-7051
E-mail: Zimei.Bu@fccc.edu

Mark R. Chance
Professor
Department of Physiology & Biophysics
Case Western Reserve University
930 BRB, 10900 Euclid Ave.
Cleveland, OH 44106
Phone: (216) 368-4406
E-mail: mark.chance@case.edu

Tom Irving
Professor of Biology and Physics
Dept. BCPS
Illinois Institute of Technology
3101 S. Dearborn
Chicago, IL 60616
Phone: (312) 567-3489
E-mail: irving@agni.phys.iit.edu

Hiro Tsuruta
Senior Scientist
Stanford Synchrotron Radiation Laboratory
Stanford Linear Accelerator Center
2575 Sand Hill Road, MS 69
Menlo Park, CA 94025-7015
Phone: (650)926-3104
E-mail: tsuruta@slac.stanford.edu

NOTE: This same proposal team is also submitting a LOI for an instrument for high throughput, static protein solution scattering measurements, which could be either a side branch on this beamline, or the three-pole wiggler beamline sharing the same sector with this one.

NSLS-II Beamline Letter of Intent

Title	A highly automated instrument for static X-ray scattering measurements of biological molecules in solution.
Science Program	Highly automated data collection and analysis of solution scattering data for biophysical characterization of enzymes, membrane proteins, RNA and DNA, and interactions in macromolecular assemblies, in support of functional characterization in structural genomics efforts and ligand discovery in chemical genetics and drug development.
Beamline Description	Small- and wide-angle X-ray scattering at a fixed X-ray energy (12keV), with a TPW source, or share the undulator source with the high brightness biological X-ray scattering beamline.
Proposal Type	Type 1

Proposal Team (the membership is expected to evolve as the proposal is being developed)

Lin Yang (Spokesperson)
Scientist
National Synchrotron Light Source
Brookhaven National Laboratory
Upton, NY 11973
Phone: (631) 344-5833
E-mail: lyang@bnl.gov

Marc Allaire
Biophysicist
National Synchrotron Light Source
Brookhaven National Laboratory
Upton, NY 11973
Phone: (631) 344-4795
E-mail: allaire@bnl.gov

Zimei Bu
Associate Member
Fox Chase Cancer Center
Reimann 414, 333 Cottman Ave
Philadelphia, PA 19111-2434
Phone: (215) 728-7051
E-mail: Zimei.Bu@fccc.edu

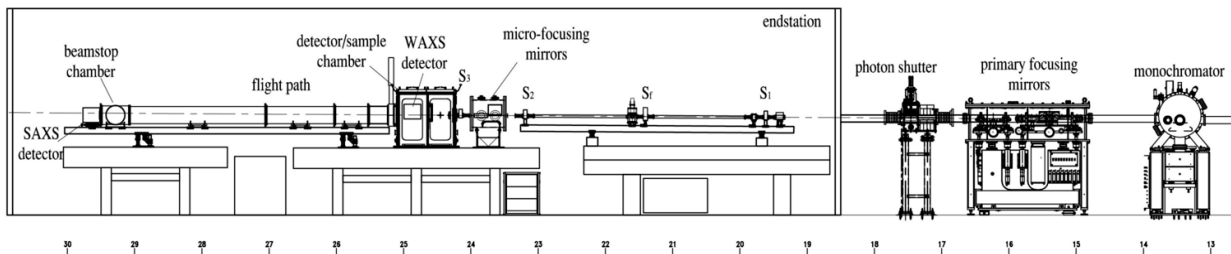
Mark R. Chance
Professor
Department of Physiology & Biophysics
Case Western Reserve University
930 BRB, 10900 Euclid Ave.
Cleveland, OH 44106
Phone: (216) 368-4406
E-mail: mark.chance@case.edu

Tom Irving
Professor of Biology and Physics
Dept. BCPS
Illinois Institute of Technology
3101 S. Dearborn
Chicago, IL 60616
Phone: (312) 567-3489
E-mail: irving@agni.phys.iit.edu

Hiro Tsuruta
Senior Scientist
Stanford Synchrotron Radiation
Laboratory
Stanford Linear Accelerator Center
2575 Sand Hill Road, MS 69
Menlo Park, CA 94025-7015
Phone: (650)926-3104
E-mail: tsuruta@slac.stanford.edu

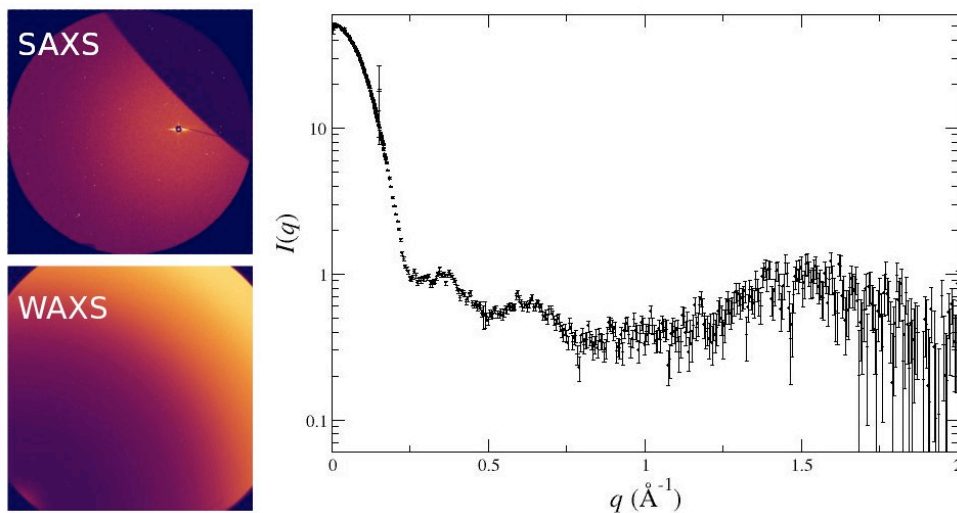
NOTE: This same proposal team is also submitting an LOI for a high brightness X-ray scattering beamline for biological applications. Since the science programs on these two beamlines will be closely related, the source for this instrument ideally should be the three-pole wiggler in the same sector with the undulator-based high brightness beamline. Alternatively, the two beamlines can also share the same undulator source, with optional future upgrade for this beamline to have its own short undulator source.

Appendix II. Layout of beamline X9 and representative SAXS/WAXS data



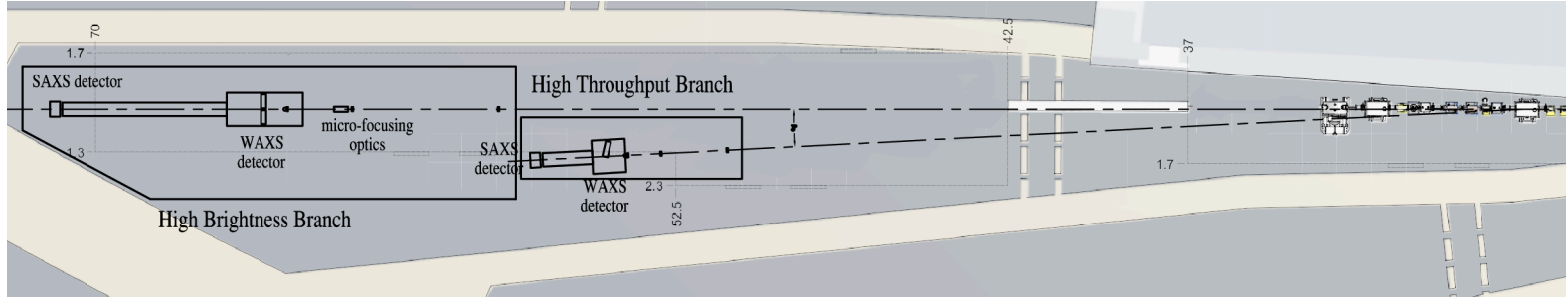
The X9 beamline utilizes two sets of focusing mirrors to achieve flexible control of the beam size and divergence. The primary focusing mirror system is based on adaptive mirrors and can focus the beam to any location in the endstation. When microbeam is required, the beam is first focused on to slits S_f . The micro-focusing mirrors then image this secondary source to the sample position within the detector/sample chamber.

Two detectors are used routinely in data collection. The SAXS detector is located at the end of the flight path, up to 5m from the sample, while the WAXS detector is located in the detector/sample chamber, at ~ 30 cm from the sample. The typical scattering patterns and the combined 1D data in solution scattering measurements, from a 3.8mg/ml lysozyme sample, are shown below.



The micro-focusing mirror pair can be individually (horizontal and vertical) moved in or out of the beam to switch between configurations that require focused beam and those that do not. Several beamstop are available in the beamstop chamber to be used for either transmission or grazing incident measurements.

Appendix III. Possible layout of two instruments sharing the same ID port



Given that the scientific programs hosted by these two instruments are closely related, it may be beneficial to build these instruments as two branches on the same ID port, operated by the same group of beamline staff that have the expertise to support these experiments. Doing so also may also result in some savings in terms of operation and equipment cost. The high throughput branch can be offset from the high brightness branch by ~ 3 degrees using a single-bounce multilayer monochromator, followed by a channel-cut Si(111) monochromator to reduce the flux of the side-bounced beam. The source of the high throughput branch can be a short undulator canted from the standard undulator that serves the high brightness branch. Alternatively, the two branches could also use the same source and operate mutually exclusively.

Appendix IV: Choice of source

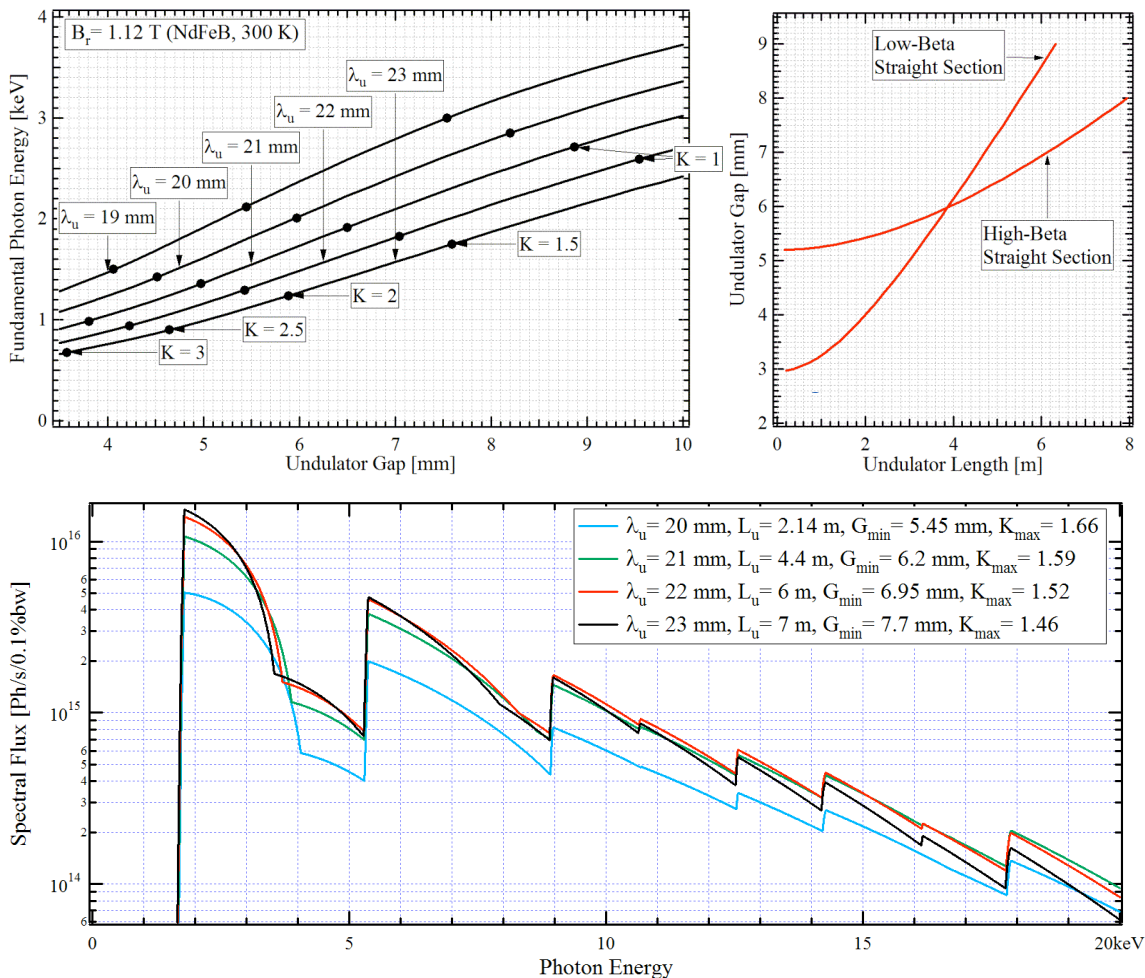
1. High brightness instrument

NSLS-II will have standard designs of undulators utilizing similar magnetic structures but with different length of magnetic periods. Several issues need to be taken into account when choosing the undulator source.

The tuning curves for these standard undulators have a gap near 4keV, between the fundamental and the 3rd harmonic of the undulator radiation. Within this gap, the 2nd harmonic radiation can still be utilized, at brightness more than one order of magnitude lower than beyond the gap. The width of this gap is determined by the maximum of the achievable undulator deflection parameter, K_{\max} . The higher the K_{\max} , the narrower the gap, since the fundamental X-ray energy of the undulator radiation is given by

$$\lambda_1 = \frac{1 + K^2/2}{2\gamma^2} \lambda_u,$$

where λ_u is the magnetic period of the undulator. The deflection parameter for an undulator of given magnetic material is given by $K \sim 0.936\lambda_u B_r \exp(-\pi g/\lambda_u)$, where g

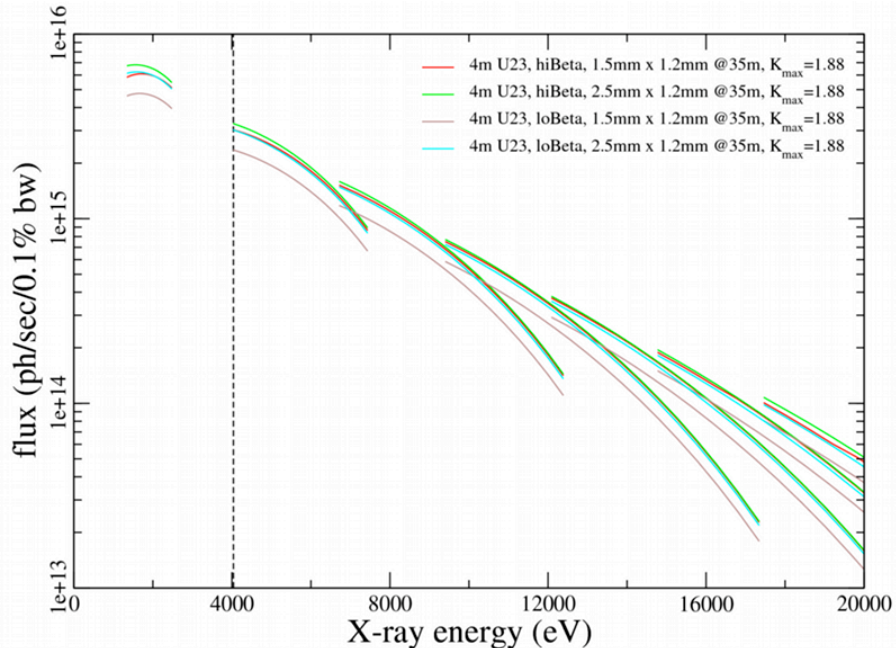


Source: Q. Shen presentation, NSLS-II information session, see <http://www.bnl.gov/nsls2/2010BeamlineProposals.asp>

(mm) is the undulator gap and B_r (T) is the remnant field of the magnets. Therefore it is desirable to have an undulator of longer periods (e.g. U22 rather than U20).

The electron orbit in the storage ring sets constraints to the minimum gap at which the undulator is allowed to operate. This constraint is dependent upon the beta function (high-beta vs. low-beta) of the straight section in which the undulator is located. In general a shorter undulator is allowed to close the gap more. In addition, for an undulator of given length, the gap can be closed more to achieve higher K in a low-beta straight section when the undulator is less than ~ 4 m long, whereas the opposite is true if the undulator is longer than 4m. A 4m-long U23 undulator is feasible in both types of straight sections and able to provide access to 4keV X-rays (near the K-edge of Ca).

For the 3 beamline configurations considered in this document, only the 1-micron beam configuration require a high-brightness source rather than a high-flux one (in this configuration both the size and the divergence of the secondary source must be trimmed). Furthermore the samples that will be measured in this configuration will likely produce high scattering intensity (periodic structures). Therefore a high-flux source (high-beta) is preferred for this instrument, based on the flux that is captured by the primary focusing mirrors as shown below.



The long high-beta straight section may also be able to accommodate an additional undulator as the independent source for the high throughput branch. The options are more limited in a low-beta straight section due to its shorter length.

2. High throughput instrument

In general an undulator is the preferred source for an SAXS instrument because of its low X-ray beam divergence. The arc source provided by NSLS-II for hard X-ray beamlines is the three-pole wiggler (TPW). It has similar flux performance compared to the NSLS bending magnet. A multilayer monochromator with high bandwidth is therefore required

to provide improved flux for protein solution scattering experiments. With the TPW source, the estimated flux at the sample will be 1.8×10^{12} photon/sec, assuming 50% multilayer reflectivity. In comparison, the flux at the sample using a 15-period version of the U20 undulator (148 periods) and Si(111) monochromator will be 1.6×10^{12} photons/sec.

Appendix IV. Optical design for micron-beam SAXS

In order to achieve nearly rectangular beam intensity profile at the sample position, it is useful to utilize the following two-stage focusing scheme. The primary focusing mirrors first focus the beam onto a set of slits. Using the slits as the source, the secondary focusing optics then re-focus the beam to the sample position. The size of the beam at the sample position can be adjusted by setting the size of the slits.

With ideal mirrors, the "brightness" (intensity / (size x divergence)) of the source would be conserved at the image plane. However, current technology can only achieve 0.3-0.5 μ rad RMS slope error for mirrors that are long enough (>0.5m long) to capture the central cone of undulator radiation. The brightness of the secondary source will be therefore worse than that of the undulator source. Note that the relative contribution to the beam size by the mirror slope error is independent of the image side focal length. This is apparent if this contribution is compared to the undistorted beam size at the source plane. The degradation of photon beam brightness due to mirror slope error is therefore also independent of the image side focal length of the primary focusing mirror.

In the second focusing stage, the beam size and divergence at the sample set the constraints for the optics design. In the most demanding case, the beam size of 1 micorn and lowest q of 0.005\AA^{-1} are required. The lowest q in turn sets the limit of beam divergence to 0.4mrad (1mm at 2.5m, safety factor of 4). Assume that the micro-focusing optics will be mirrors that are 20cm long with RMS slope error of 0.1 μ rad. At 3mrad incident angle, the optical aperture of each mirror will be 0.6mm. The optimal working distance will be therefore $0.6\text{mm}/0.4\text{mrad} = 1.5\text{m}$, corresponding to the diffraction-limited beam size of 0.17 μm and the slope error-limited beam size of 0.3 μm . In order to achieve precise control on the beam size at the sample, it is convenient to choose a relatively large demagnification, say 10, for the secondary focusing optics. The source side focal length will be therefore 15m.

Given the space limitation, the image side focal length for the primary focusing mirrors will be 13m, with demagnification of ~ 2.7 . And the slope error contribution to the beam size will be $\sim 2 \times 0.3 \mu\text{rad} \times 13\text{m} \sim 8\mu\text{m}$. The resulted size and divergence of the secondary source, as compared to those for the undulator source, are listed below (photon beam at 10keV, based on Fig. 5 in NSLS-II SourceProperties.pdf). Note that the effective brightness of the secondary source is degraded more by the mirror slope error when the source size is smaller.

Type of source	Low- β 3m U20				High- β 6m U22				Required sec. src (full size)
	E beam	Ph. src	Beam @35m (4σ)	Sec. src	E beam	Ph. src.	Beam @35m (4σ)	Sec. src	
σ_h (μm)	33.3	34	2.5mm	14	107	110	1.2mm	41	10
σ_h' (μrad)	16.5	18		49	5.1	8		22	40
σ_v (μm)	2.9	7	1.1mm	8	5.2	13	1.0mm	9	10
σ_v' (μrad)	2.7	8		22	1.5	7		19	40

The figure of the focusing mirrors should be adjustable, either by mechanical benders or by utilizing biomorph mirrors. Depending on the required beam size and divergence at the sample, the location of the secondary source, or the locations of the independent vertical and horizontal secondary sources, can be varied to achieve optimal flux at the sample. The configurations used for flux estimates in the text are listed below.

Undulator source: 4m U23, K=1.89, E=12keV

Primary focusing mirrors:

VFM @ 35 m, 0.4 m long, 0.3 micro-rad RMS slope error

HFM @ 36 m, 0.85 m long, 0.3 micro-rad RMS slope error

Secondary focusing mirrors:

mVFM @ 62.8 m, 0.2 m long, 0.1 micro-rad RMS slope error

mHFM @ 63 m, 0.2 m long, 0.1 micro-rad RMS slope error

Sample @ 64.5 m

Detector @ 67 m

All mirrors are positioned at 3 mrad incident angle.

Configuration #1:

Target beam size at the sample:

~ 25 micron (FWHM, H) x 5 micron (full beam, V)

Secondary sources

high-beta: @ 55 m (H) and 53 m (V)

low-beta: @ 59 m (H) and 55 m (V)

Demagnification

high-beta: 1.89 x 5.33 (H) and 1.94 x 5.76 (V)

low-beta: 1.57 x 2.67 (H) and 1.75 x 4.59 (V)

Slit size for secondary source

high-beta: 0.25mm (H) x 24 micron (V)

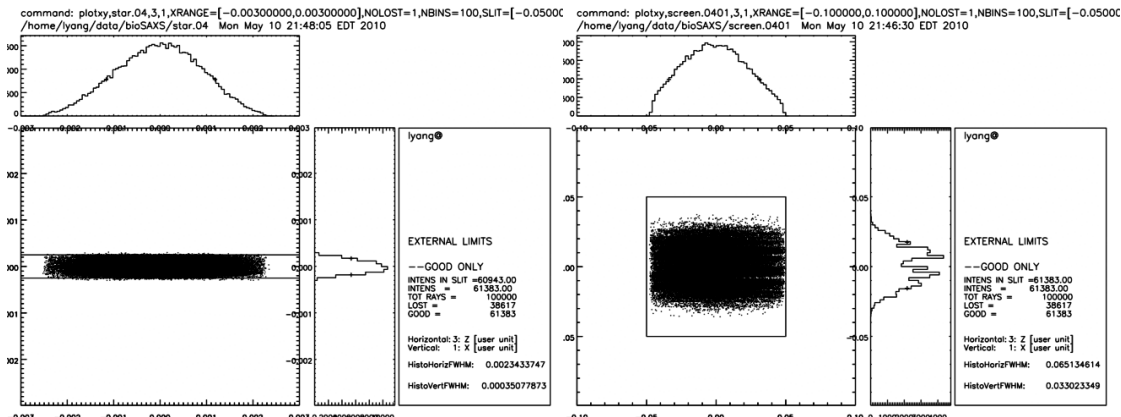
low-beta: 0.13mm (H) x 20 micron (V)

Expected vertical spot size (from source size and demagnification):

high-beta: 4.2 microns low-beta: 4.4 microns

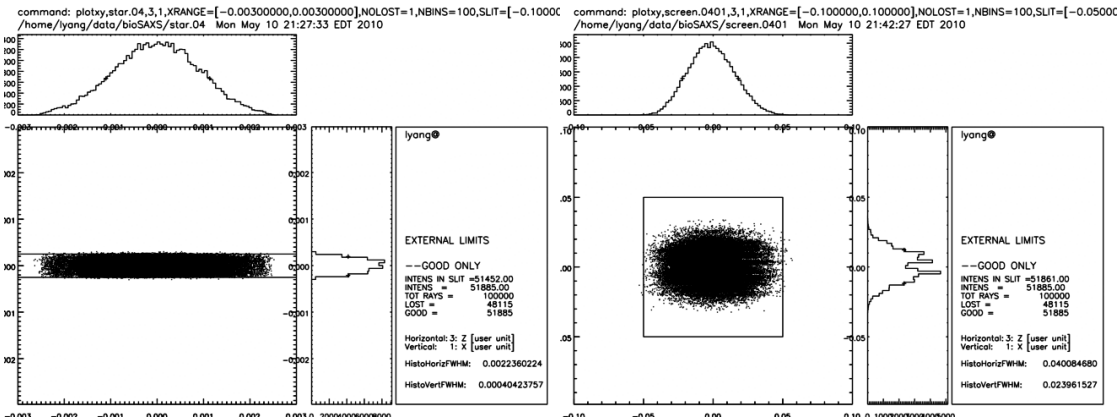
Shadow simulation results for high-beta: 61% good rays, 2.4×10^{13} photons/sec/0.01%bw (left) Beam at the sample. The box is 5 microns high.

(right) Beam at the detector. The box is 1mm x 1mm.



** FOCUSING ELEMENTS **					** DISTANCES FOR ALL O.E. [cm] **				
OE	SHAPE	p_foc	q_foc	1/M	OE	TYPE	p[cm]	q[cm]	to src
1	ELLIPSE	3500.00	1800.00	1.94	1	MIRROR	3500.00	50.00	3550.00
2	ELLIPSE	3600.00	1900.00	1.89	2	MIRROR	50.00	1700.00	5300.00
3	ELLIPSE	980.00	170.00	5.76	3	MIRROR	980.00	10.00	6290.00
4	ELLIPSE	800.00	150.00	5.33	4	MIRROR	10.00	150.00	6450.00

Low-beta: 52% good rays, 2.0×10^{13} photons/sec/0.01%bw



** FOCUSING ELEMENTS **					** DISTANCES FOR ALL O.E. [cm] **				
OE	SHAPE	p_foc	q_foc	1/M	OE	TYPE	p[cm]	q[cm]	to src
1	ELLIPSE	3500.00	2000.00	1.75	1	MIRROR	3500.00	50.00	3550.00
2	ELLIPSE	3600.00	2300.00	1.57	2	MIRROR	50.00	1900.00	5500.00
3	ELLIPSE	780.00	170.00	4.59	3	MIRROR	780.00	10.00	6290.00
4	ELLIPSE	400.00	150.00	2.67	4	MIRROR	10.00	150.00	6450.00

Comments: The flux at the sample is not really limited by the brightness of the source. High flux source gives higher flux at the sample as well.

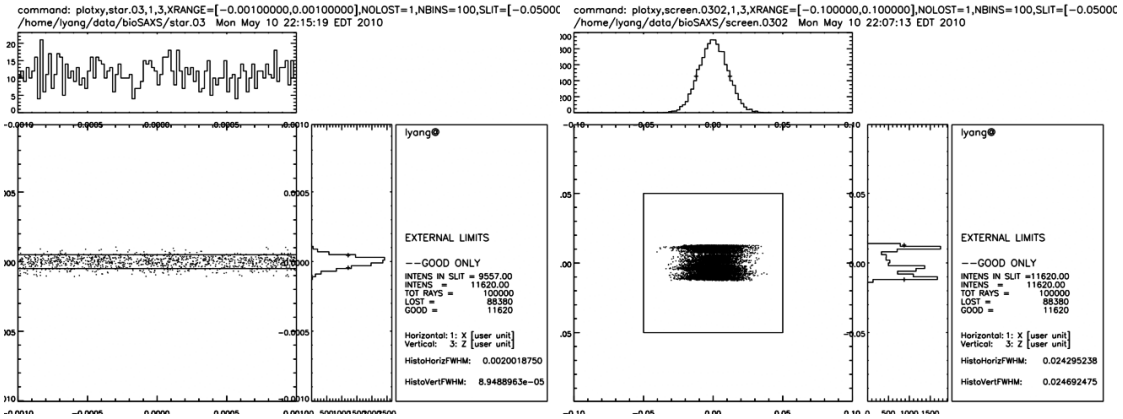
Configuration #2:

- Target beam size at the sample: 1 micron (FWHM), vertical only
- Secondary source @ 50 m (vertical only)
- Demagnification: 1.26 (H, focus to the sample) and 2.33 x 8.67 (V)
- Slit size for secondary source: 9 micron (vertical only)
- Divergence limiting aperture: 0.15 mm (vertical only)
- [should consider moving HFM upstream of VFM to get lower vertical divergence]

High beta: 11.6% good rays, 4.5×10^{12} photons/sec/0.01%bw

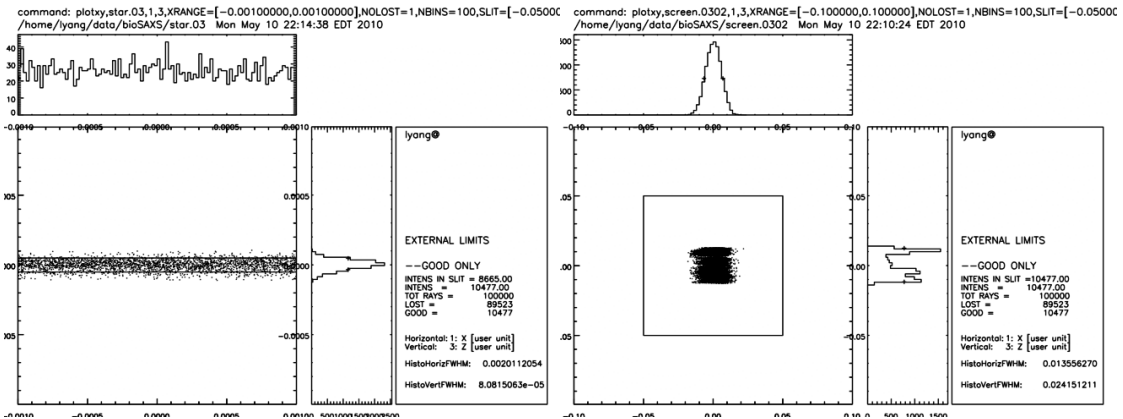
(left) Beam at the sample. The box is 1 microns high.

(right) Beam at the detector. The box is 1mm x 1mm.



** FOCUSING ELEMENTS **					** DISTANCES FOR ALL O.E. [cm] **				
OE	SHAPE	p_foc	q_foc	1/M	OE	TYPE	p[cm]	q[cm]	to src
1	ELLIPSE	3500.00	1500.00	2.33	1	MIRROR	3500.00	50.00	3550.00
2	ELLIPSE	3600.00	2850.00	1.26	2	MIRROR	50.00	1400.00	5000.00
3	ELLIPSE	1300.00	150.00	8.67	3	MIRROR	1300.00	150.00	6450.00

Low beta: 10.5% good rays, 4.1×10^{12} photons/sec/0.01%bw



** FOCUSING ELEMENTS **					** DISTANCES FOR ALL O.E. [cm] **				
OE	SHAPE	p_foc	q_foc	1/M	OE	TYPE	p[cm]	q[cm]	to src
1	ELLIPSE	3500.00	1500.00	2.33	1	MIRROR	3500.00	50.00	3550.00
2	ELLIPSE	3600.00	2850.00	1.26	2	MIRROR	50.00	1400.00	5000.00
3	ELLIPSE	1300.00	150.00	8.67	3	MIRROR	1300.00	150.00	6450.00

Comments: The flux at the sample is limited by source brightness in the vertical direction only. The horizontal beam size is larger in the high-beta case (200 microns at the sample vs. 75 microns for low-beta). But the horizontal beam size is not important for the intended membrane structure experiments and can be adjusted easily.

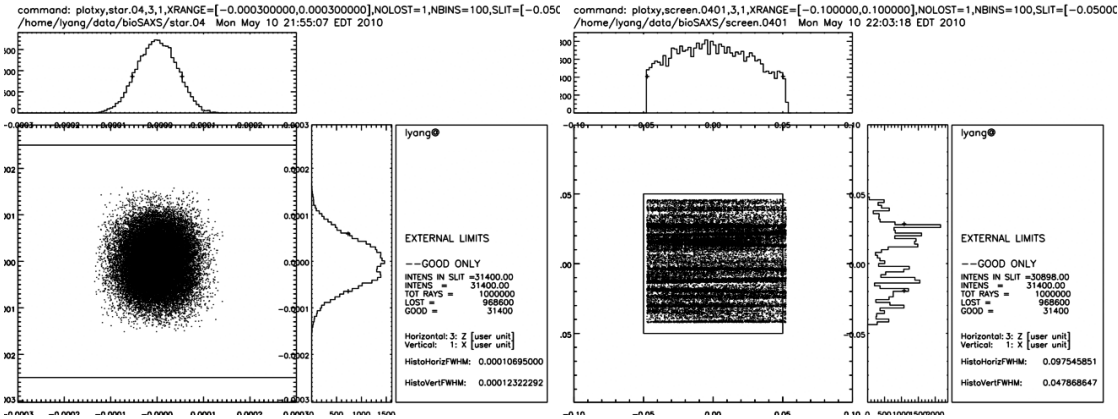
Configuration #3:

Target beam size at the sample: 1 micron x 1 micron (FWHM)

Secondary source @ 48 m

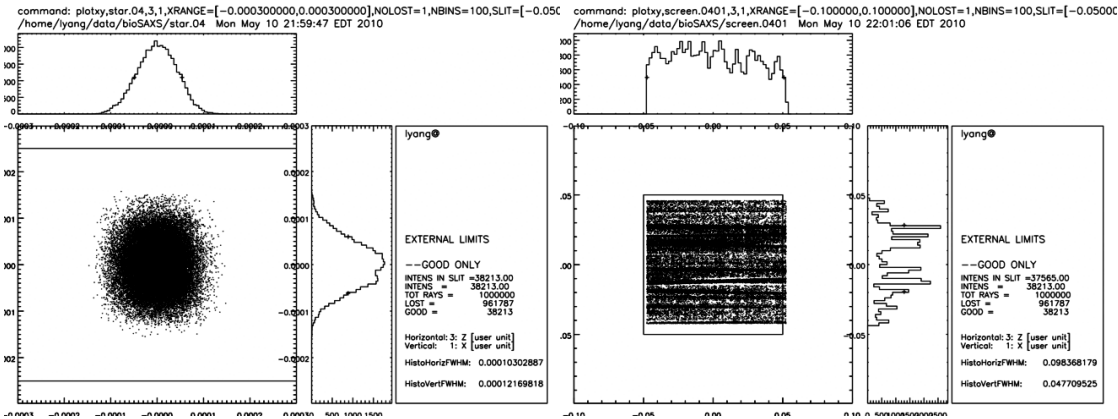
Demagnification: 3×10 (H) and 2.69×8.71 (V)
 Slit size for secondary source: 10 micron x 10 micron

High-beta: 3.1% good rays, 1.2×10^{12} photons/sec/0.01%bw
 (left) Beam at the sample. The box is 5 microns high.
 (right) Beam at the detector. The box is 1mm x 1mm.



** FOCUSING ELEMENTS **					** DISTANCES FOR ALL O.E. [cm] **				
OE	SHAPE	p_foc	q_foc	1/M	OE	TYPE	p[cm]	q[cm]	to src
1	ELLIPSE	3500.00	1300.00	2.69	1	MIRROR	3500.00	50.00	3550.00
2	ELLIPSE	3600.00	1200.00	3.00	2	MIRROR	50.00	1200.00	4800.00
3	ELLIPSE	1480.00	170.00	8.71	3	MIRROR	1480.00	10.00	6290.0
4	ELLIPSE	1500.00	150.00	10.00	4	MIRROR	10.00	150.00	6450.00

Low-beta: 3.8% good rays, 1.5×10^{12} photons/sec/0.01%bw



** FOCUSING ELEMENTS **					** DISTANCES FOR ALL O.E. [cm] **				
OE	SHAPE	p_foc	q_foc	1/M	OE	TYPE	p[cm]	q[cm]	to src
1	ELLIPSE	3500.00	1300.00	2.69	1	MIRROR	3500.00	50.00	3550.00
2	ELLIPSE	3600.00	1200.00	3.00	2	MIRROR	50.00	1200.00	4800.00
3	ELLIPSE	1480.00	170.00	8.71	3	MIRROR	1480.00	10.00	6290.00
4	ELLIPSE	1500.00	150.00	10.00	4	MIRROR	10.00	150.00	6450.00

Comments: In this case the flux at the sample is limited by source brightness in both horizontal and vertical directions. The brighter low-beta source gives higher flux at the sample.